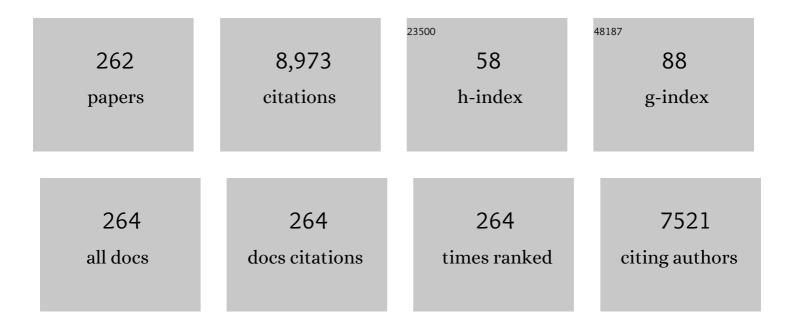
List of Publications by Year in descending order

Source: https://exaly.com/author-pdf/6762713/publications.pdf Version: 2024-02-01



IOHN KENNEDY

#	Article	IF	CITATIONS
1	Effect of Ag doped MnO2 nanostructures suitable for wastewater treatment and other environmental pollutant applications. Environmental Research, 2022, 205, 112560.	3.7	77
2	Reproducibility and long-term stability of Sn doped MnO2 nanostructures: Practical photocatalytic systems and wastewater treatment applications. Chemosphere, 2022, 293, 133646.	4.2	48
3	Tailoring of magnetic anisotropy by ion irradiation for magnetic tunnel junction sensors. Journal of Alloys and Compounds, 2022, 910, 164902.	2.8	8
4	Doping and defect engineering induced extremely high magnetization and large coercivity in Co doped MoTe2. Journal of Alloys and Compounds, 2022, 918, 165750.	2.8	7
5	The role of sulfur valency on thermoelectric properties of sulfur ion implanted copper iodide. Journal of Alloys and Compounds, 2022, 921, 166103.	2.8	4
6	lon Beam Analysis of Proton-Induced X-ray Emission (PIXE) Techniques for Elemental Investigation of Young Stage Neem Leaf of Southern India, Tamil Nadu. Biological Trace Element Research, 2021, 199, 3540-3546.	1.9	12
7	Preparation and characterization of ion beam sputtered graphitic carbon nitride thin film. Materials Today: Proceedings, 2021, 36, 488-491.	0.9	3
8	Effect of surface nanopatterning on the thermoelectric properties of bismuth antimony telluride films. Materials Today: Proceedings, 2021, 36, 416-420.	0.9	5
9	Fabrication of superparamagnetic permalloy nanostructures in ZnO matrix by ion beam sputtering. Materials Today: Proceedings, 2021, 36, 582-586.	0.9	3
10	Magnetisation and magnetic anisotropy of ion beam synthesised iron nitride. Journal of Magnetism and Magnetic Materials, 2021, 517, 167388.	1.0	5
11	The effect of low energy helium implantation on the structural, vibrational, and piezoelectric properties of AlN thin films. Physica B: Condensed Matter, 2021, 601, 412481.	1.3	7
12	Tuning the electromechanical properties and polarization of Aluminium Nitride by ion beam-induced point defects. Acta Materialia, 2021, 203, 116495.	3.8	11
13	A facile route to insulate an Fe-based nanocrystalline alloy powder for magnetic composite cores. Materials Science and Engineering B: Solid-State Materials for Advanced Technology, 2021, 264, 114928.	1.7	5
14	Role of phase separation in nanocomposite indium-tin-oxide films for transparent thermoelectric applications. Journal of Materiomics, 2021, 7, 612-620.	2.8	28
15	The electronic properties and defect chemistry of Bi2-xSe3, –0.05 <x<0.15. 109752.<="" 148,="" 2021,="" and="" chemistry="" journal="" of="" physics="" solids,="" td=""><td>1.9</td><td>4</td></x<0.15.>	1.9	4
16	Effect of native defects on thermoelectric properties of copper iodide films. Emergent Materials, 2021, 4, 761-768.	3.2	25
17	Evolution of Rutherford's ion beam science to applied research activities at GNS Science. Journal of the Royal Society of New Zealand, 2021, 51, 574-591.	1.0	7
18	A review on sustainable recycling technologies for lithium-ion batteries. Emergent Materials, 2021, 4, 725-735.	3.2	33

#	Article	IF	CITATIONS
19	Giant Piezoelectricity of Deformed Aluminum Nitride Stabilized through Noble Gas Interstitials for Energy Efficient Resonators. Advanced Electronic Materials, 2021, 7, 2100358.	2.6	5
20	Effect of long-term stability of the aluminium nitride - silicon interface for microwave-frequency electronic devices. Applied Surface Science, 2021, 551, 149461.	3.1	8
21	Ironsand (Titanomagnetite-Titanohematite): Chemistry, Magnetic Properties and Direct Applications for Wireless Power Transfer. Materials, 2021, 14, 5455.	1.3	4
22	Multifold enhancements in thermoelectric power factor in isovalent sulfur doped bismuth antimony telluride films. Materials Research Bulletin, 2021, 142, 111426.	2.7	23
23	Hybrid anode materials for rechargeable batteries a€" A review of Sn/HO <mml:math xmlns:mml="http://www.w3.org/1998/Math/MathML" display="inline" id="d1e2027" altimg="si44.svg"><mml:msub><mml:mrow /><mml:mrow><mml:mn>2</mml:mn></mml:mrow></mml:mrow </mml:msub> based nanocomposites.</mml:math 	2.5	17
24	Energy Reports, 2021, 7, 2836-2848. Enhancing the piezoelectric modulus of wurtzite AlN by ion beam strain engineering. Applied Physics Letters, 2021, 118, .	1.5	8
25	Defects Engineering Induced Ultrahigh Magnetization in Rare Earth Element Ndâ€doped MoS ₂ . Advanced Quantum Technologies, 2021, 4, 2000093.	1.8	19
26	High Coercivity and Magnetization in WSe ₂ by Codoping Co and Nb. Small, 2020, 16, e1903173.	5.2	43
27	The Itinerant 2D Electron Gas of the Indium Oxide (111) Surface: Implications for Carbon―and Energy onversion Applications. Small, 2020, 16, e1903321.	5.2	17
28	A tensile technique for measuring frozen products adhesion strength: Application to stainless steel/frozen milk interaction. Journal of Food Engineering, 2020, 271, 109772.	2.7	5
29	High performance of pyrochlore like Sm2Ti2O7 heterojunction photocatalyst for efficient degradation of rhodamine-B dye with waste water under visible light irradiation. Journal of King Saud University - Science, 2020, 32, 1516-1522.	1.6	150
30	Influence of Carrier Density and Energy Barrier Scattering on a High Seebeck Coefficient and Power Factor in Transparent Thermoelectric Copper Iodide. ACS Applied Energy Materials, 2020, 3, 10037-10044.	2.5	49
31	Investigation of structural and electrical properties of lithium cobalt oxide nanoparticles for optoelectronic applications. Surfaces and Interfaces, 2020, 20, 100582.	1.5	13
32	Structural and electrical properties of Mg-doped vanadium dioxide thin films via room-temperature ion implantation. Surfaces and Interfaces, 2020, 20, 100590.	1.5	7
33	Colossal Magnetization and Giant Coercivity in Ion-Implanted (Nb and Co) MoS ₂ Crystals. ACS Applied Materials & Interfaces, 2020, 12, 58140-58148.	4.0	22
34	Influence of solvent and precursor concentration on the properties of NiV2O6 nanoparticles. Surfaces and Interfaces, 2020, 21, 100711.	1.5	5
35	Studies of MnO2/g-C3N4 hetrostructure efficient of visible light photocatalyst for pollutants degradation by sol-gel technique. Surfaces and Interfaces, 2020, 20, 100512.	1.5	112
36	Low leakage Mg-compensated GaN Schottky diodes on free-standing GaN substrate for high energy \$alpha\$-particle detection. , 2020, , .		0

3

#	Article	IF	CITATIONS
37	Remarkable thermal conductivity enhancement in Ag—decorated graphene nanocomposites based nanofluid by laser liquid solid interaction in ethylene glycol. Scientific Reports, 2020, 10, 10982.	1.6	25
38	Electrical and chemical stability of CuS nanofluids for conductivity of water soluble based nanocomposites. Surfaces and Interfaces, 2020, 19, 100475.	1.5	11
39	Influence of C-implanted ions on the transition properties of VO2 thin films. MRS Advances, 2020, 5, 2139-2146.	0.5	3
40	Enhanced thermal conductivity of nanofluids made of metal oxide nanostructures synthesized by arc discharge method. International Journal of Modern Physics B, 2020, 34, 2040001.	1.0	1
41	Investigation of New Zealand's natural magnetic minerals for application in inroad charging systems. International Journal of Modern Physics B, 2020, 34, 2040018.	1.0	5
42	Photocatalytic oxygen evolution reaction for energy conversion and storage of functional nanomaterials. , 2020, , 55-81.		3
43	Catalyst-free synthesis of copper oxide composites as solar radiative filters. Nanotechnology, 2020, 31, 504002.	1.3	5
44	Vertical GaN-on-GaN Schottky Diodes as α-Particle Radiation Sensors. Micromachines, 2020, 11, 519.	1.4	17
45	Exchange bias and large room temperature magnetoresistance in ion beam-synthesized Co nanoparticles in SiO2. Emergent Materials, 2019, 2, 313-325.	3.2	9
46	Secondary phase induced electrical conductivity and improvement in thermoelectric power factor of zinc antimonide films. Materials Today Energy, 2019, 13, 249-255.	2.5	32
47	A comparison of traditional manufacturing vs additive manufacturing, the best method for the job. Procedia Manufacturing, 2019, 30, 11-18.	1.9	233
48	Effects of surface topography and chemistry modifications of stainless steel through ion implantation on icephobicity. Procedia Manufacturing, 2019, 30, 231-238.	1.9	4
49	Observation of multiple magnetic phases and complex nanostructures in Co implanted amorphous carbon films. Journal of Physics and Chemistry of Solids, 2019, 127, 158-163.	1.9	6
50	Improved photocatalytic decomposition of aqueous Rhodamine-B by solar light illuminated hierarchical yttria nanosphere decorated ceria nanorods. Journal of Materials Research and Technology, 2019, 8, 2898-2909.	2.6	104
51	Stalling behaviour of chloride ions: A non-enzymatic electrochemical detection of α-Endosulfan using CuO interface. Sensors and Actuators B: Chemical, 2019, 293, 100-106.	4.0	107
52	Low Voltage High-Energy α-Particle Detectors by GaN-on-GaN Schottky Diodes with Record-High Charge Collection Efficiency. Sensors, 2019, 19, 5107.	2.1	10
53	Multifold improvement of thermoelectric power factor by tuning bismuth and antimony in nanostructured n-type bismuth antimony telluride thin films. Materials and Design, 2019, 163, 107549.	3.3	61
54	Decorative black coatings on titanium surfaces based on hard bi-layered carbon coatings synthesized by carbon implantation. Surface and Coatings Technology, 2019, 358, 386-393.	2.2	14

#	Article	IF	CITATIONS
55	The effect of different Fe concentrations on the structural and magnetic properties of near surface superparamagnetic Ni1â°Fe nanoparticles in SiO2 made by dual low energy ion implantation. Journal of Magnetism and Magnetic Materials, 2019, 473, 125-130.	1.0	13
56	ZnO doped single wall carbon nanotube as an active medium for gas sensor and solar absorber. Journal of Materials Science: Materials in Electronics, 2019, 30, 147-158.	1.1	88
57	Structural and chemical changes of cellulose fibres under low energy ion implantations. Surface and Coatings Technology, 2018, 355, 191-199.	2.2	8
58	Antibacterial, magnetic, optical and humidity sensor studies of β-CoMoO 4 - Co 3 O 4 nanocomposites and its synthesis and characterization. Journal of Photochemistry and Photobiology B: Biology, 2018, 183, 233-241.	1.7	152
59	Spin-dependent tunnelling in magnetite nanoparticles. Journal of Magnetism and Magnetic Materials, 2018, 460, 229-233.	1.0	97
60	Structural and magnetic properties of near surface superparamagnetic Ni1-Fe nanoparticles in SiO2 formed by low energy dual ion implantation with different fluences. Applied Surface Science, 2018, 449, 399-404.	3.1	5
61	Titania Solid Thin Films Deposited by ppâ€MOCVD Exhibiting Visible Light Photocatalytic Activity. Physica Status Solidi (A) Applications and Materials Science, 2018, 215, 1700578.	0.8	2
62	An analog method of cross-talk compensation for a RGB wavelength division multiplexed optical link. Optics and Laser Technology, 2018, 102, 85-92.	2.2	0
63	Magnetic properties of Co doped WSe2 by implantation. Journal of Alloys and Compounds, 2018, 731, 25-31.	2.8	40
64	Structure and morphology of copper oxide composite materials synthesized by the arc discharge method. Modern Physics Letters B, 2018, 32, 1840067.	1.0	4
65	The effect of reheating layers in Metal Additive Manufacturing on the external surface finish of a printed part. , 2018, , .		0
66	28Si+ ion beams from Penning ion source based implanter systems for near-surface isotopic purification of silicon. Review of Scientific Instruments, 2018, 89, 123305.	0.6	17
67	Evaluation on La2O3 garlanded ceria heterostructured binary metal oxide nanoplates for UV/ visible light induced removal of organic dye from urban wastewater. South African Journal of Chemical Engineering, 2018, 26, 49-60.	1.2	124
68	Laser-Induced Breakdown Spectroscopy (LIBS) on Geological Samples: Compositional Differentiation. MRS Advances, 2018, 3, 1969-1983.	0.5	7
69	Enhanced Power Factor and Increased Conductivity of Aluminum Doped Zinc Oxide Thin Films for Thermoelectric Applications. Journal of Nanoscience and Nanotechnology, 2018, 18, 1384-1387.	0.9	43
70	Photocatalytic decomposition effect of erbium doped cerium oxide nanostructures driven by visible light irradiation: Investigation of cytotoxicity, antibacterial growth inhibition using catalyst. Journal of Photochemistry and Photobiology B: Biology, 2018, 185, 275-282.	1.7	155
71	Equilibrium and kinetic studies of the adsorption of acid blue 9 and Safranin O from aqueous solutions by MgO decked FLG coated Fuller's earth. Journal of Physics and Chemistry of Solids, 2018, 123, 43-51.	1.9	127
72	Design of intelligent surfaces for energy intensive processing industry. MATEC Web of Conferences, 2018, 185, 00001.	0.1	3

#	Article	IF	CITATIONS
73	Effect of annealing high-dose heavy-ion irradiated high-temperature superconductor wires. Nuclear Instruments & Methods in Physics Research B, 2017, 409, 351-355.	0.6	6
74	Defects engineering induced room temperature ferromagnetism in transition metal doped MoS 2. Materials and Design, 2017, 121, 77-84.	3.3	97
75	High performance symmetric supercapacitor based on zinc hydroxychloride nanosheets and 3D graphene-nickel foam composite. Applied Surface Science, 2017, 405, 329-336.	3.1	133
76	Hydrogen-related excitons and their excited-state transitions in ZnO. Physical Review B, 2017, 95, .	1.1	29
77	Structural, optical and magnetic investigation of Gd implanted CeO2 nanocrystals. Nuclear Instruments & Methods in Physics Research B, 2017, 409, 147-152.	0.6	86
78	Can sodium silicates affect collagen structure during tanning? Insights from small angle X-ray scattering (SAXS) studies. RSC Advances, 2017, 7, 11665-11671.	1.7	14
79	The effect of fluence on the magnetic properties of superparamagnetic iron-nickel nanoparticles in SiO2 made by dual Ni and Fe low energy ion implantation. Nuclear Instruments & Methods in Physics Research B, 2017, 409, 187-191.	0.6	3
80	Enhanced magnetic properties of polymer-magnetic nanostructures synthesized by ultrasonication. Journal of Alloys and Compounds, 2017, 720, 395-400.	2.8	76
81	Antiproliferative effects on human lung cell lines A549 activity of cadmium selenide nanoparticles extracted from cytotoxic effects: Investigation of bio-electronic application. Materials Science and Engineering C, 2017, 76, 1012-1025.	3.8	133
82	In vitro cytotoxicity effect and antibacterial performance of human lung epithelial cells A549 activity of Zinc oxide doped TiO 2 nanocrystals: Investigation of bio-medical application by chemical method. Materials Science and Engineering C, 2017, 74, 325-333.	3.8	223
83	Synthesis and enhanced field emission of zinc oxide incorporated carbon nanotubes. Diamond and Related Materials, 2017, 71, 79-84.	1.8	113
84	Multiferroic nanocrystalline BiFeO _{3 and BiCrO_{3 thin films prepared by ion beam sputtering. International Journal of Nanotechnology, 2017, 14, 56.}}	0.1	9
85	Inducing High Coercivity in MoS ₂ Nanosheets by Transition Element Doping. Chemistry of Materials, 2017, 29, 9066-9074.	3.2	81
86	Excess oxygen limited diffusion and precipitation of iron in amorphous silicon dioxide. Journal of Applied Physics, 2017, 122, .	1.1	3
87	Evaluation on the heterostructured CeO2/Y2O3 binary metal oxide nanocomposites for UV/Vis light induced photocatalytic degradation of Rhodamine - B dye for textile engineering application. Journal of Alloys and Compounds, 2017, 727, 1324-1337.	2.8	222
88	Improved planar device isolation in AlGaN/GaN HEMTs on Si by ultra-heavy 131 Xe+ implantation. Physica Status Solidi (A) Applications and Materials Science, 2017, 214, 1600794.	0.8	6
89	Positioning of cobalt atoms in amorphous carbon films by pre-selecting the hydrogen concentration. Nuclear Instruments & Methods in Physics Research B, 2017, 409, 116-120.	0.6	3
90	Nickel nanowires mesh fabricated by ion beam irradiation-induced nanoscale welding for transparent conducting electrodes. Materials Research Express, 2017, 4, 075042.	0.8	16

#	Article	IF	CITATIONS
91	Molecular carbon nitride ion beams for enhanced corrosion resistance of stainless steel. Nuclear Instruments & Methods in Physics Research B, 2017, 409, 86-90.	0.6	3
92	Elucidation of photocatalysis, photoluminescence and antibacterial studies of ZnO thin films by spin coating method. Journal of Photochemistry and Photobiology B: Biology, 2017, 173, 466-475.	1.7	218
93	Improved, Photon Conversion Efficiency of (SnO2) Doped Cesium Oxide (Cs) Nanofibers for Photocatalytic Application Under Solar Irradiation. Springer Proceedings in Physics, 2017, , 113-128.	0.1	5
94	AlGaN/GaN high electron mobility transistors on Si with sputtered TiN gate. Physica Status Solidi (A) Applications and Materials Science, 2017, 214, 1600555.	0.8	15
95	Photocatalytic activity of ZrO 2 doped lead dioxide nanocomposites: Investigation of structural and optical microscopy of RhB organic dye. Applied Surface Science, 2017, 421, 234-239.	3.1	128
96	Nanocrystalline multiferroic BiFeO3 thin films made by room temperature sputtering and thermal annealing, and formation of an iron oxide-induced exchange bias. Journal of Alloys and Compounds, 2017, 695, 3061-3068.	2.8	30
97	A fundamental study of 3D printing testing methods for the development of new quality management strategies. , 2017, , .		5
98	Soil property spatial & temporal variability sensing for precision agriculture. , 2017, , .		0
99	Synthesis of magnetic nanoparticles by low-energy dual ion implantation of iron and nickel into silicon dioxide followed by electron beam annealing. International Journal of Nanotechnology, 2017, 14, 348.	0.1	0
100	Development of Quality Management Strategies for 3D Printing Testing Methods $\hat{a} \in \hat{~}$ a Review. , 2017, , .		1
101	Rice Husks As A Sustainable Source Of High Quality Nanostructured Silica For High Performance Li-ionÂbattery Requital By Sol-gel Method – A Review. Advanced Materials Letters, 2016, 7, 684-696.	0.3	65
102	High spin-dependent tunneling magnetoresistance in magnetite powders made by arc-discharge. Journal of Applied Physics, 2016, 120, .	1.1	78
103	Photodegradation of organic pollutants RhB dye using UV simulated sunlight on ceria based TiO2 nanomaterials for antibacterial applications. Scientific Reports, 2016, 6, 38064.	1.6	353
104	Ni1â^'xFex nanoparticles made by low energy dual ion implantation into SiO2. Materials Research Express, 2016, 3, 126102.	0.8	4
105	Thermally stable device isolation by inert gas heavy ion implantation in AlGaN/GaN HEMTs on Si. Journal of Vacuum Science and Technology B:Nanotechnology and Microelectronics, 2016, 34, 042203.	0.6	22
106	Formation of magnetic nanoparticles by low energy dual implantation of Ni and Fe into SiO2. Journal of Alloys and Compounds, 2016, 667, 255-261.	2.8	82
107	Solution processing of CuSe quantum dots: Photocatalytic activity under RhB for UV and visible-light solar irradiation. Materials Science and Engineering B: Solid-State Materials for Advanced Technology, 2016, 210, 1-9.	1.7	151
108	Poly(dimethylsiloxane) grafted with adhesive polymeric chains provide a route towards cost effective dry adhesives. European Polymer Journal, 2016, 84, 13-21.	2.6	3

#	Article	IF	CITATIONS
109	Synthesis and analytical applications of photoluminescent carbon nanosheet by exfoliation of graphite oxide without purification. Journal of Materials Science: Materials in Electronics, 2016, 27, 13080-13085.	1.1	72
110	Photoluminescence of well-aligned ZnO doped CeO2 nanoplatelets by a solvothermal route. Materials Letters, 2016, 183, 351-354.	1.3	103
111	Fugitive emissions from nanopowder manufacturing. Journal of Nanoparticle Research, 2016, 18, 1.	0.8	3
112	Controlling preferred orientation and electrical conductivity of zinc oxide thin films by post growth annealing treatment. Applied Surface Science, 2016, 367, 52-58.	3.1	229
113	Structural, optical and morphological properties of post-growth calcined TiO2 nanopowder for opto-electronic device application: Ex-situ studies. Journal of Alloys and Compounds, 2016, 671, 486-492.	2.8	58
114	Synthesis and characterization studies of NiO nanorods for enhancing solar cell efficiency using photon upconversion materials. Ceramics International, 2016, 42, 8385-8394.	2.3	195
115	Bioinspired dry adhesive: Poly(dimethylsiloxane) grafted with poly(2-ethylhexyl acrylate) brushes. European Polymer Journal, 2015, 68, 432-440.	2.6	10
116	Nanomechanical and in situ TEM characterization of boron carbide thin films on helium implanted substrates: Delamination, real-time cracking and substrate buckling. Materials Science & Engineering A: Structural Materials: Properties, Microstructure and Processing, 2015, 639, 54-64.	2.6	6
117	Microstructural, electrical and magnetic properties of erbium doped zinc oxide single crystals. Electronic Materials Letters, 2015, 11, 998-1002.	1.0	30
118	Synthesis and Compositional Analysis of Permalloy Powder Prepared by Arc-Discharge. Journal of Nanoscience and Nanotechnology, 2015, 15, 9612-9616.	0.9	9
119	Effective Low-Temperature Flux Pinning by Au Ion Irradiation in HTS Coated Conductors. IEEE Transactions on Applied Superconductivity, 2015, 25, 1-5.	1.1	17
120	Nonlinear effects in defect production by atomic and molecular ion implantation. Journal of Applied Physics, 2015, 117, .	1.1	4
121	Antibacterial effect of silver nanofilm modified stainless steel surface. International Journal of Modern Physics B, 2015, 29, 1540013.	1.0	9
122	Hybrid nanostructured thin-films by PLD for enhanced field emission performance for radiation micro-nano dosimetry applications. Journal of Alloys and Compounds, 2015, 647, 141-145.	2.8	83
123	A comparative study on the morphological features of highly ordered MgO:AgO nanocube arrays prepared <i>via</i> a hydrothermal method. RSC Advances, 2015, 5, 82421-82428.	1.7	110
124	Structural, electronic and magnetic properties of Er implanted ZnO thin films. Nuclear Instruments & Methods in Physics Research B, 2015, 359, 1-4.	0.6	11
125	Enhanced visible photoluminescent and structural properties of ZnO/KIT-6 nanoporous materials for white light emitting diode (w-LED) application. Journal of Alloys and Compounds, 2015, 651, 479-482.	2.8	87
126	Instability of Hydrogenated TiO ₂ . Journal of Physical Chemistry Letters, 2015, 6, 4627-4632.	2.1	48

#	Article	IF	CITATIONS
127	Diabetic cardiomyopathy is associated with defective myocellular copper regulation and both defects are rectified by divalent copper chelation. Cardiovascular Diabetology, 2014, 13, 100.	2.7	57
128	Enhancement of the magnetic properties of iron nanoparticles upon incorporation of samarium. Materials Research Express, 2014, 1, 026110.	0.8	2
129	Quantum confinement and photoluminescence of well-aligned CdO nanofibers by a solvothermal route. Materials Letters, 2014, 120, 243-245.	1.3	88
130	One dimensional well-aligned CdO nanocrystal by solvothermal method. Journal of Alloys and Compounds, 2014, 593, 67-70.	2.8	157
131	Investigations of near infrared reflective behaviour of TiO2 nanopowders synthesized by arc discharge. Optical Materials, 2014, 36, 1260-1265.	1.7	42
132	Applications of nanoparticle-based fluxgate magnetometers for positioning and location. , 2014, , .		6
133	Large magnetoresistance in a permalloy/Ba2FeMoO6 sputtered film. Physica B: Condensed Matter, 2014, 436, 126-129.	1.3	2
134	Improved device isolation in AlGaN/GaN HEMTs on Si by heavy Kr ⁺ Ion implantation. , 2014, , .		4
135	Investigation of structural and photoluminescence properties of gas and metal ions doped zinc oxide single crystals. Journal of Alloys and Compounds, 2014, 616, 614-617.	2.8	211
136	Epitaxial zinc oxide, graphene oxide composite thin-films by laser technique for micro-Raman and enhanced field emission study. Ceramics International, 2014, 40, 16065-16070.	2.3	134
137	Effects of annealing on the structural and optical properties of zinc sulfide thin films deposited by ion beam sputtering. Materials Science in Semiconductor Processing, 2014, 26, 561-566.	1.9	69
138	Influence of filter thickness on PESA calibration. Nuclear Instruments & Methods in Physics Research B, 2014, 332, 445-448.	0.6	2
139	Enhanced reduction of silicon oxide thin films on silicon under electron beam annealing. Nuclear Instruments & Methods in Physics Research B, 2014, 332, 421-425.	0.6	2
140	Synthesis and structural, magnetic and magnetotransport properties of permalloy powders containing nanoparticles prepared by arc discharge. Journal of Alloys and Compounds, 2014, 608, 153-157.	2.8	18
141	Magneto-resistance study of AFe _{2As_{2 (A = Sr, Ba) iron-based compounds. International Journal of Nanotechnology, 2014, 11, 403.}}	0.1	1
142	Structural and chemical changes during the growth of Fe nanoparticles in SiO _{2 under low energy ion implantation. International Journal of Nanotechnology, 2014, 11, 466.}	0.1	4
143	Polymer brushes for improvement of dry adhesion in biomimetic dry adhesives. International Journal of Nanotechnology, 2014, 11, 636.	0.1	5
144	Structural and Compositional Characterization of Ion Beam Sputtered Hydroxyapatite Thin Films on Ti-6Al-4V. Asian Journal of Applied Sciences, 2014, 7, 745-752.	0.4	4

#	Article	IF	CITATIONS
145	Contamination of PDMS microchannels by lithographic molds. Lab on A Chip, 2013, 13, 4312.	3.1	15
146	Use of micro-proton elastic scattering analysis to determine water content in geological powders. Nuclear Instruments & Methods in Physics Research B, 2013, 306, 257-260.	0.6	3
147	Magnetic-ion-doped silicon nanostructures fabricated by ion implantation and electron beam annealing. Nuclear Instruments & Methods in Physics Research B, 2013, 307, 131-136.	0.6	Ο
148	Protection of the heart by treatment with a divalent-copper-selective chelator reveals a novel mechanism underlying cardiomyopathy in diabetic rats. Cardiovascular Diabetology, 2013, 12, 123.	2.7	38
149	Al2O3 coatings on stainless steel using pulsed-pressure MOCVD. Surface and Coatings Technology, 2013, 230, 208-212.	2.2	15
150	Atomic retention and near infrared photoluminescence from PbSe nanocrystals fabricated by sequential ion implantation and electron beam annealing. Nuclear Instruments & Methods in Physics Research B, 2013, 307, 154-157.	0.6	9
151	Intrinsic magnetic order and inhomogeneous transport in Gd-implanted zinc oxide. Physical Review B, 2013, 88, .	1.1	99
152	Correlation between microstructural and magnetic properties of Tb implanted ZnO. AIP Conference Proceedings, 2013, , .	0.3	7
153	Large low-temperature magnetoresistance in SrFe ₂ As ₂ single crystals. Europhysics Letters, 2013, 104, 17002.	0.7	11
154	ZnO nanostructures synthesized by arc discharge for optical coating and sensor applications. , 2013, , .		1
155	Transition metal doped metal oxide nanostructures synthesized by arc discharge method. , 2013, , .		0
156	SYNTHESIS OF Mg DOPED TiO2 NANOCRYSTALS PREPARED BY WET-CHEMICAL METHOD: OPTICAL AND MICROSCOPIC STUDIES. International Journal of Nanoscience, 2013, 12, 1350033.	0.4	76
157	Iron-based bimagnetic core/shell nanostructures in SiO2: a TEM, MEIS, and energy-resolved XPS analysis. Journal of Nanoparticle Research, 2012, 14, 1.	0.8	11
158	Influence of Doping on Hybrid Organic–Inorganic WO3(4,4′-bipyridyl)0.5 Materials. Journal of Physical Chemistry C, 2012, 116, 3787-3792.	1.5	6
159	Field Emission Characteristics ofSnO2/CNTs Composites Prepared by Microwave-Assisted Wet Impregnation. Journal of Nanomaterials, 2012, 2012, 1-4.	1.5	5
160	Modifying the conductivity of polypyrrole through low-energy lead ion implantation. Materials Chemistry and Physics, 2012, 136, 903-909.	2.0	6
161	Observation of magnetism, low resistivity, and magnetoresistance in the near-surface region of Gd implanted ZnO. Applied Physics Letters, 2012, 101, 082408.	1.5	64
162	Tailoring the Conductivity of Polypyrrole Films Using Low-Energy Platinum Ion Implantation. Journal of Physical Chemistry C, 2012, 116, 8236-8242.	1.5	15

#	Article	IF	CITATIONS
163	Ionâ€beam synthesis of 3C‣iC surface layers on silicon. Surface and Interface Analysis, 2012, 44, 399-404.	0.8	1
164	Morphology and characterization of TiO2 nanoparticles synthesized by arc discharge. Chemical Physics Letters, 2012, 521, 86-90.	1.2	66
165	Enhancement of wettability and antibiotic loading/release of hydroxyapatite thin film modified by 100MeV Ag7+ ion irradiation. Materials Chemistry and Physics, 2012, 134, 464-477.	2.0	41
166	Structural and magnetic properties of low-energy Gd implanted ZnO single crystals. Nuclear Instruments & Methods in Physics Research B, 2012, 272, 100-103.	0.6	21
167	High temperature annealing effects on low energy iron implanted SiO2. Nuclear Instruments & Methods in Physics Research B, 2012, 273, 182-185.	0.6	6
168	Formation of nanoclusters with varying Pb/Se concentration and distribution after sequential Pb+ and Se+ ion implantation into SiO2. Nuclear Instruments & Methods in Physics Research B, 2012, 273, 199-202.	0.6	6
169	Evolution of the structure and magneto-optical properties of ion beam synthesized iron nanoclusters. Journal of Materials Science, 2012, 47, 1127-1134.	1.7	11
170	Effect of annealing on the structural, electrical and magnetic properties of Gd-implanted ZnO thin films. Journal of Materials Science, 2012, 47, 1119-1126.	1.7	69
171	Sensors based on metal oxide nanostructures synthesized by arc discharge. , 2011, , .		3
172	Nucleation and Growth of Fe Nanoparticles in SiO ₂ : A TEM, XPS, and Fe L-Edge XANES Investigation. Journal of Physical Chemistry C, 2011, 115, 20978-20985.	1.5	122
173	Surface superconductivity on SrFe ₂ As ₂ single crystals induced by ion implantation. Europhysics Letters, 2011, 94, 37009.	0.7	7
174	Size-controlled synthesis and gas sensing application of tungsten oxide nanostructures produced by arc discharge. Nanotechnology, 2011, 22, 335702.	1.3	73
175	High conductivity transparent carbon nanotube films deposited from superacid. Nanotechnology, 2011, 22, 309502.	1.3	3
176	A study on the redistribution of ion-implanted nitrogen in Ti-modified austenitic steel. Journal of Nuclear Materials, 2011, 414, 382-385.	1.3	4
177	Fabrication of surface magnetic nanoclusters using low energy ion implantation and electron beam annealing. Nanotechnology, 2011, 22, 115602.	1.3	67
178	Large room temperature magnetoresistance in ion beam synthesized surface Fe nanoclusters on SiO2. Applied Physics Letters, 2011, 98, .	1.5	55
179	Structural and photoluminescence properties of Gd implanted ZnO single crystals. Journal of Applied Physics, 2011, 110, .	1.1	76
180	Characterization of the Structural and Electrical Properties of Ion Beam Sputtered ZnO Films. Materials Science Forum, 2011, 700, 49-52.	0.3	9

#	Article	IF	CITATIONS
181	Annealing Behavior of Ion-implanted Nitrogen in D9 Steel. AIP Conference Proceedings, 2011, , .	0.3	1
182	Electron Beam Annealing of Fe+ Implanted Si Nanostructures. Journal of Nanoscience and Nanotechnology, 2010, 10, 6556-6561.	0.9	4
183	Modulation of Field Emission Properties of ZnO Nanorods During Arc Discharge. Journal of Nanoscience and Nanotechnology, 2010, 10, 8239-8243.	0.9	53
184	Identification of a Deep Acceptor Level in ZnO Due to Silver Doping. Journal of Electronic Materials, 2010, 39, 577-583.	1.0	17
185	Field Emission from Silicon Implanted with Carbon and Nitrogen Followed by Electron Beam Annealing. Journal of Electronic Materials, 2010, 39, 1262-1267.	1.0	0
186	Epitaxial Growth and Electrical Properties of Thick SmSi2Layers on (001) Silicon. Japanese Journal of Applied Physics, 2010, 49, 025505.	0.8	5
187	Properties of nitrogen implanted and electron beam annealed bulk ZnO. Journal of Applied Physics, 2010, 107, .	1.1	70
188	Synthesis and structure of Na+-intercalated WO3(4,4′-bipyridyl)0.5. Chemical Communications, 2010, 46, 4261.	2.2	8
189	Fluxâ€Pinning Centers In Metalâ€Organic Deposited YBCO Coated Conductors. AIP Conference Proceedings, 2009, , .	0.3	4
190	Unique photoluminescence from ZnO grown by eclipse pulsed laser deposition. Journal of Vacuum Science & Technology B, 2009, 27, 1698.	1.3	5
191	Compositional and Structural Study of Gd Implanted ZnO Films. , 2009, , .		4
192	Flux pinning by discontinuous columnar defects in 74MeV Ag-irradiated YBa2Cu3O7 coated conductors. Physica C: Superconductivity and Its Applications, 2009, 469, 2060-2067.	0.6	46
193	UV and humidity sensing properties of ZnO nanorods prepared by the arc discharge method. Nanotechnology, 2009, 20, 245502.	1.3	231
194	Group-IV and V ion implantation into nanomaterials and elemental analysis on the nanometre scale. International Journal of Nanotechnology, 2009, 6, 369.	0.1	66
195	Sub-surface retention of Pb atoms in silicon after low-energy ion implantation and electron beam annealing. Nuclear Instruments & Methods in Physics Research B, 2008, 266, 1553-1557.	0.6	5
196	Ion beam analysis of rare earth nitride thin films. Nuclear Instruments & Methods in Physics Research B, 2008, 266, 1558-1561.	0.6	8
197	A copper(II)-selective chelator ameliorates diabetes-evoked renal fibrosis and albuminuria, and suppresses pathogenic TGF-Î ² activation in the kidneys of rats used as a model of diabetes. Diabetologia, 2008, 51, 1741-1751.	2.9	62
198	Nanostructuring at the surface of low-energy lead-implanted silicon by electron beam annealing. Surface and Interface Analysis, 2008, 40, 931-934.	0.8	6

#	Article	IF	CITATIONS
199	Mg doping of InN and the use of yttriumâ€stabilised zirconia substrates. Physica Status Solidi C: Current Topics in Solid State Physics, 2008, 5, 508-510.	0.8	4
200	Carbon enhanced blue–violet luminescence in ZnO films grown by pulsed laser deposition. Current Applied Physics, 2008, 8, 283-286.	1.1	44
201	Raman scattering investigation of hydrogen and nitrogen ion implanted ZnO thin films. Current Applied Physics, 2008, 8, 291-294.	1.1	66
202	Self-assembled germanium nanostructures formed using electron-beam annealing. Current Applied Physics, 2008, 8, 276-279.	1.1	7
203	PIXE ANALYSIS OF COPPER, CHROMIUM AND ARSENIC DISTRIBUTIONS IN CCA-TREATED TIMBER. International Journal of PIXE, 2008, 18, 261-266.	0.4	2
204	PIXE ANALYSIS OF SEDIMENTS AFFECTED BY THE DECEMBER 2004 INDIAN OCEAN TSUNAMI. International Journal of PIXE, 2008, 18, 227-240.	0.4	5
205	Depth Profiling of N and C in Ion Implanted ZnO and Si Using Deuterium Induced Nuclear Reaction Analysis. , 2008, , .		1
206	Enhanced Flux Pinning in MOD Second Generation HTS Wires by Silver- and Copper-Ion Irradiation. IEEE Transactions on Applied Superconductivity, 2007, 17, 3306-3309.	1.1	7
207	Characteristics of hetero-junction diodes based on ion beam sputtered ZnO thin films. , 2007, , .		3
208	Development of a Network-Wide Harmonic Control Scheme Using an Active Filter. IEEE Transactions on Power Delivery, 2007, 22, 1847-1856.	2.9	13
209	Digital Business Ecosystems (DBE). , 2007, , .		1
210	Elemental analysis of urban stormwater particulate matter by PIXE. Nuclear Instruments & Methods in Physics Research B, 2007, 258, 435-439.	0.6	4
211	Mobility of copper, chromium and arsenic from treated timber into grapevines. Science of the Total Environment, 2007, 388, 35-42.	3.9	28
212	Ion Beam Analysis of Amorphous and Nanocrystalline Group III-V Nitride and ZnO Thin Films. Journal of Electronic Materials, 2007, 36, 472-482.	1.0	63
213	Oxygen uptake of InN thin films as determined by ion beam analysis. Thin Solid Films, 2007, 515, 3736-3739.	0.8	5
214	Microprobe analysis of brine shrimp grown on meteorite extracts. Nuclear Instruments & Methods in Physics Research B, 2007, 260, 184-189.	0.6	4
215	Deuteron microprobe analysis of carbon in the transition region between SiC and Si nanostructures grown on Si. Nuclear Instruments & Methods in Physics Research B, 2007, 260, 325-328.	0.6	1
216	Atom ingress from synthetic body fluid into nanoporous layers formed in titanium by helium ion-implantation. Current Applied Physics, 2006, 6, 327-330.	1.1	2

#	Article	IF	CITATIONS
217	Modification of electrical conductivity in RF magnetron sputtered ZnO films by low-energy hydrogen ion implantation. Current Applied Physics, 2006, 6, 495-498.	1.1	62
218	Formation of large SiC nanocrystals on Si(100) by 12C implantation and electron beam annealing. Current Applied Physics, 2006, 6, 507-510.	1.1	9
219	A nuclear reaction analysis and optical microscopy study on controlled growth of large SiC nanocrystals on Si formed by low-energy ion implantation and electron beam annealing. Nuclear Instruments & Methods in Physics Research B, 2006, 249, 105-108.	0.6	3
220	Photoluminescence, Capacitance-Voltage, and Variable Field Hall Effect Measurements of Mg-Doped InN. Materials Research Society Symposia Proceedings, 2006, 955, 1.	0.1	0
221	Single phase nanocrystalline GaMnN thin films with high Mn content. Journal of Applied Physics, 2006, 100, 084310.	1.1	12
222	CHARACTERIZATION OF ZnO FILMS BY ION BEAM ANALYSIS. International Journal of Modern Physics B, 2006, 20, 4655-4660.	1.0	5
223	Optical and compositional properties of indium nitride grown by plasma assisted molecular beam epitaxy. Smart Materials and Structures, 2006, 15, S87-S91.	1.8	2
224	Co2MnX (XSi, Ge, Sn, SbSn) thin films grown by pulsed-laser deposition. Journal of Crystal Growth, 2005, 275, e1183-e1188.	0.7	6
225	Polycrystalline InGaN grown by MBE on fused silica glass. Physica Status Solidi C: Current Topics in Solid State Physics, 2005, 2, 2236-2239.	0.8	6
226	Magnetic and optical properties of the InCrN system. Journal of Applied Physics, 2005, 98, 043903.	1.1	32
227	Optical conductivity and x-ray absorption and emission study of the band structure of MnN films. Physical Review B, 2005, 72, .	1.1	11
228	Quantitative study of molecularN2trapped in disordered GaN:O films. Physical Review B, 2004, 70, .	1.1	32
229	Minority-spin band parameters in a NiMnSb thin film determined by spectral conductivity. Journal of Applied Physics, 2004, 96, 6421-6424.	1.1	2
230	Structural and optical properties of indium nitride grown by plasma-assisted molecular beam epitaxy. , 2004, , .		4
231	SUPPRESSION OF SILICON NANOSTRUCTURE GROWTH BY MEDIUM ENERGY NITROGEN ION IMPLANTATION. International Journal of Nanoscience, 2004, 03, 431-437.	0.4	1
232	SiC nanoboulders on silicon – a nuclear reaction analysis study of low energy 13C implanted and subsequently electron beam annealed (100) silicon. Nuclear Instruments & Methods in Physics Research B, 2004, 217, 583-588.	0.6	16
233	Analysis of heteroepitaxial germanium on gallium arsenide grown by pulsed laser deposition. Current Applied Physics, 2004, 4, 229-232.	1.1	1
234	Optimization of Non-Fluorine Sol-Gel Derived YBCO Thin Films. Journal of Electroceramics, 2004, 13, 361-365.	0.8	1

#	Article	IF	CITATIONS
235	Depth profiling of light elements in PAMBE-grown GaN and helium-implanted titanium with heavy ion time-of-flight elastic recoil detection. Surface and Interface Analysis, 2004, 36, 317-322.	0.8	4
236	Photocatalytic titania coatings. Current Applied Physics, 2004, 4, 189-192.	1.1	71
237	Characterisation of polycrystalline gallium nitride grown by plasma-assisted evaporation. Current Applied Physics, 2004, 4, 225-228.	1.1	15
238	Plasma immersion nitrogen implantation into silicon and rapid thermal electron beam annealing for surface structuring. Current Applied Physics, 2004, 4, 241-244.	1.1	1
239	Surface smoothing of thin HTc YBa2Cu3O7â^î´ superconducting films by high-energy iodine ions. Current Applied Physics, 2004, 4, 288-291.	1.1	0
240	Carbon depth profiling of superconducting YBCO thin films on nanometer scale. Current Applied Physics, 2004, 4, 292-295.	1.1	4
241	Formation of micrometer sized crater shaped pits in silicon by low-energy 22Ne+ implantation and electron beam annealing. Nuclear Instruments & Methods in Physics Research B, 2003, 206, 179-183.	0.6	10
242	Uptake of light elements of nanoporous layers formed by helium ion implantation. Nuclear Instruments & Methods in Physics Research B, 2003, 206, 1056-1061.	0.6	7
243	Microprobe analysis of light elements in nanoporous surfaces produced by helium ion implantation. Nuclear Instruments & Methods in Physics Research B, 2003, 210, 543-547.	0.6	5
244	Optical and Microstructural Characterisation of InN Grown by PAMBE on (0001) Sapphire and (001) YSZ. Materials Research Society Symposia Proceedings, 2003, 798, 22.	0.1	2
245	Surface Dynamics of GaAs Thin Film Formation by Pulsed Laser Deposition Investigated Using RHEED. Materials Research Society Symposia Proceedings, 2002, 749, 1.	0.1	0
246	Ion beam analysis of ion-assisted deposited amorphous GaN. Nuclear Instruments & Methods in Physics Research B, 2002, 190, 620-624.	0.6	29
247	Trace element analysis of blood samples from mentally challenged children by PIXE. Nuclear Instruments & Methods in Physics Research B, 2002, 190, 449-452.	0.6	8
248	Measurement of lateral straggling using a microbeam. Nuclear Instruments & Methods in Physics Research B, 2001, 181, 157-163.	0.6	10
249	EFFECT OF ION-ENERGY ON THE PROPERTIES OF AMORPHOUS GaN FILMS PRODUCED BY ION-ASSISTED DEPOSITION. Modern Physics Letters B, 2001, 15, 1355-1360.	1.0	7
250	PROBING FOR FLUORINE IN NITRIDED SIO2 FILMS BY ION BEAM ANALYSIS. Modern Physics Letters B, 2001, 15, 1332-1338.	1.0	2
251	CHARACTERIZATION OF SUPERCONDUCTING MULTILAYERED FILMS USING RBS AND TEM. Modern Physics Letters B, 2001, 15, 1314-1320.	1.0	3
252	A PROCEDURE FOR GOLD SOLDERING USING A Si-Au ALLOY PRODUCED BY Si IMPLANTATION IN Au. Modern Physics Letters B, 2001, 15, 1339-1347.	1.0	1

#	Article	IF	CITATIONS
253	L-subshell ionisation studies of Ta, W and Pt with protons. Nuclear Instruments & Methods in Physics Research B, 2000, 161-163, 196-201.	0.6	4
254	Au–Si eutectic alloy formation by Si implantation in polycrystalline Au. Nuclear Instruments & Methods in Physics Research B, 2000, 171, 325-331.	0.6	4
255	Trace metal distribution studies in river water by PIXE. Nuclear Instruments & Methods in Physics Research B, 1999, 150, 277-281.	0.6	13
256	PIXE analysis of trace pollutants in Chaliyar river water in Malabar, India. Nuclear Instruments & Methods in Physics Research B, 1998, 134, 224-228.	0.6	9
257	L X-ray production cross sections and their ratios in Ta, W and Pt for proton impact in the energy range 2–5.2 MeV. Nuclear Instruments & Methods in Physics Research B, 1998, 134, 165-173.	0.6	11
258	Characterisation of ZnO Thin Films Grown Directly on Sapphire by PAMBE. , 0, , .		1
259	Effects of Implanted Fe ⁺ Fluences on the Growth and Magnetic Properties of Surface Nanoclusters. Materials Science Forum, 0, 700, 37-40.	0.3	2
260	Microstructure Evolution in Nitrogen Implanted Sapphire. Advanced Materials Research, 0, 275, 222-225.	0.3	0
261	Synthesis of Zinc Oxide Nanorods and their Sensing Properties. Materials Science Forum, 0, 700, 150-153.	0.3	16
262	Effect of Annealing on Microstructure of Hydroxyapatite Coatings and their Behaviours in Simulated Body Fluid. Advanced Materials Research, 0, 922, 657-662.	0.3	9